R & D NOTES

Gas Flow and Mixing Behavior in Fine-Powder Fluidized Bed

Falei Guo
Equipment Research Institute
Luoyang Petrochemical Engineering Corp.
Luoyang, People's Republic of China

Fluidized beds employing fine powders are finding increased applications in the chemical and petroleum industries. From the point of view of a chemical reaction, the degree of gas and solid mixing is of considerable importance. Gas mixing is undesirable in that it leads to lowered reaction rate and increased side reactions. Generally, the difficulty encountered in going from a small to a large fluidized bed is caused by the different behaviors of flow and mixing in laboratory and commercial units. Various models have been applied to interpret flow and mixing phenomena in beds of fluidized solids. As the superficial gas velocity is raised from a minimum fluidization, the fluidized solids go through the bubbling, slugging, turbulent, and fast-fluidization regimes. The applicability of a bubbling model is rather limited because the model includes several parameters that depend on properties of bubbles and can be obtained only in the bubbling regime. A two-phase model seems to be adequate at low gas velocities, and so does a dispersion model, as well as others. Most commercial fluidized beds using fine-powder catalysts are operated in the turbulent regime, which is characterized by rapid coalescence and break-up of bubbles and more homogeneous appearance of the bed.

Numerous experiments confirmed that macrocirculation of solids exists in fluidized beds, either up the center and down the sides or vice versa. The macrocirculation of solids may bring gas from the top of the bed to the bottom. All theoretical models are based on the assumption that the movement of rising bubbles displaces solids upward, leading to a downward movement of solids in the remainder of the bed. While many models presented in the literature fail to explain the causes of the downward movement of solids in the bed center, Nguyen et al. (1977) succeeded in developing a particular type of pattern characterized by a relatively fast, coherent stream descending near the center toward the distributor, together with a slow downward stream near the walls, in a large bed fluidized at 0.091 m/s.

The experiments discussed here have been carried out to investigate the mechanism of gas flow and mixing in fluidized beds. Two tracing techniques have been employed in this study. One is referred to as the fine-powder tracing technique, which was developed in the present investigation to observe characteristics of gas flow in a two-dimensional fluidized bed. In the other technique hydrogen was applied as tracer gas to obtain the residence time distribution (RTD) and values of dispersion efficiency of gas. A Dirac δ-function input signal of hydrogen was injected in the beds when the beds were stationary.

Experimental Procedure

The schematic diagram of the experimental apparatus is shown in Figure 1. The thermoconductivity cell from a chromatograph SP-2305 was employed as the hydrogen detector. The experimental data were treated by a CROMEMCO Z-80 computer that was connected with a solenoid valve. Two fluidized beds were installed in the experiments: a two-dimensional bed with a rectangular cross section of 31 × 1.5 cm, and a cylindrical bed of 7 cm ID. The tracer from a hydrogen bottle flowed through the solenoid valve into the bed as an impulse input. Samples were withdrawn at 0.1 or 0.2 s intervals from the bed.

The fine-powder tracing technique was applied for the observation of turbulent eddies in the two-dimensional bed. The vessel was emptied, and then a small amount of fine-powder FCC (d_p = 0–40 μm) was added to the vessel and aerated. The track of moving fine powders was visible. To aid in identification, the movement of fine powders was followed by still and cine photographs. This fine-powder stream traced the gas turbulent eddies in the empty bed in much the same way that a dye stream may be used to trace water flow. The data for the six types of distributor that were tested in gas RTD experiments are summarized in Table 1.

The experiments were carried out under different bed depths H_o and different gas velocities u_f. Before tests, the probe connected with the thermoconductivity cell was installed under the distributor near the hydrogen injection nozzle, at which end a small disk was located to disperse the hydrogen injected into the gas stream. A method to estimate the mean residence time of

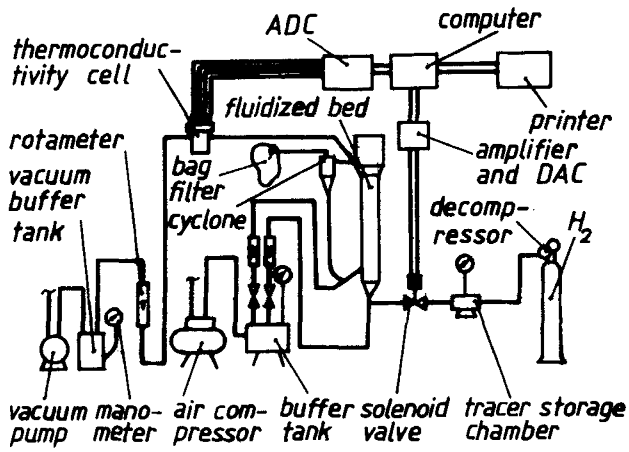

Figure 1. Experimental apparatus.

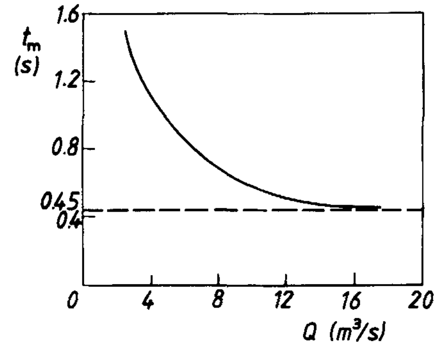

Figure 2. Determination of mean residence time of tracer in measuring system.

tracer in the measuring system is shown in Figure 2. Therefore the actual average gas velocity in the bed is:

$$u_f = \frac{H_t}{\bar{t} - \bar{t}_m} \tag{1}$$

The physical properties of fresh FCC powders used in the present experiments are summarized in Table 2.

Results and Conclusions

It was reported that even in beds with a small diameter the bubbling and turbulent fluidization regimes give rise to a structure dominated by the downward flow of solids close to the wall and a faster moving gas flowing upward through the core. In the present experiments the gas turbulent eddies just above the distributor were photographed at different gas velocities in the empty vessel by means of the fine-powder tracing technique, as shown in Figures 3, 4, and 5. The simplified models of the macroturbulent eddies in the two-dimensional bed are illustrated in Figure 6. In the case when an amount of catalyst powder was added to the vessel and the bed depth appeared, the macroturbulent eddies were distorted by gas/solid mixture because the mixture of gas and solid seemed to have much higher viscosity than a pure gas flow. The photographs indicated that there is a gas flow field above the distributor, which tends to produce either macroturbulent eddies or macrocirculation of solids in the beds. An appearance of either turbulent eddies or macrocirculation of solids in beds depends on the viscosity of the beds. The macroturbulent eddies were easily produced in the two-dimensional bed by the low viscosity, while only a macrocirculation of solids was observed at higher bed viscosity.

The shape of macroturbulent eddies in the two-dimensional bed is shown in Figures 3–5. It was observed in the experiments that the direction of rotation of the macroturbulent eddies depends on the free area ratio f_a and the shape of the distributor. With f_a = 0.3% (distributor type A), the turbulent eddies rotate in such a way that the central gas stream flows downward, and flows upward in the region at the wall. The direction of rotation of the turbulent eddies depends on the free area ratio, as indicated in the figures. It has been observed by means of the fine-powder tracing technique that the macroturbulent eddies appear symmetrically at u_f = 0.2–0.4 m/s and unsymmetrically at higher gas velocity.

Large bubbles or slugs in a turbulent bed are always broken up into smaller ones that coalesce and split. The observation in the experiments reported here supported the assumptions that the breakdown of bubbles is caused by turbulent eddies rather than by the rising movement and displacement of bubbles themselves, and that neither the bubbling model nor the diffusion process imposed on piston flow of gas (Gilliland and Mason, 1949, 1952) can interpret the gas backmixing in the turbulent regime of fluidized solids.

The gas RTD curves in the two-dimensional bed and in a bed with an inside diameter of 7 cm are demonstrated in Figures 7 and 8. A comparison of the RTD curves under different depths of the bed is illustrated in Figure 9. Both ends of the experimen-

Table 1. Data for Distributors in Two-dimensional Bed

Type	Free Area Ratio %	Orifice Data Dia. mm	No.	Arrangement
O	0.3	1	17	Equal spacing
A	1	2	14	Equal spacing
B	1	2	14	Smaller spacing in bed center
C	1	2	14	Smaller spacing in bed center
D	2	3	12	Equal spacing
E	5	3	32	Equal spacing

Table 2. Size Distribution of FCC Particles

Size Range μm	Weight %
9.8–12.4	1.24
12.4–15.6	2.29
15.6–19.7	0.95
19.7–24.8	2.98
24.8–31.2	8.39
31.2–39.2	12.24
39.2–49.6	14.68
49.6–62.4	32.16
62.4–78.7	8.39
78.7–99.1	5.59
99.1–124.9	11.19

Avg. particle dia., 43.7 μm

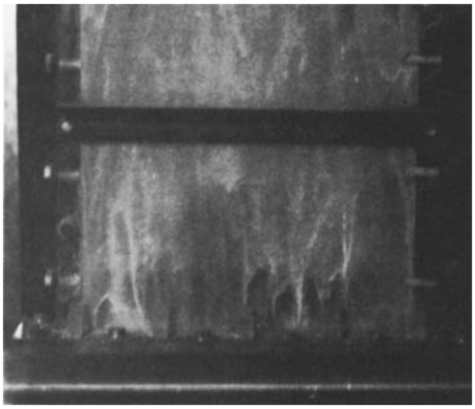

Figure 3. Macroturbulent eddies in 2D bed at $u_f = 0.124$ m/s.

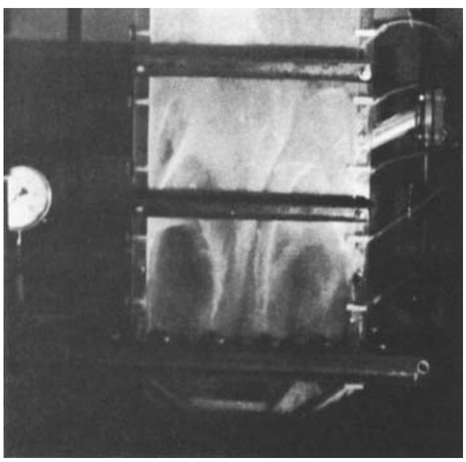

Figure 4. Macroturbulent eddies in 2D bed at $u_f = 0.310$ m/s.

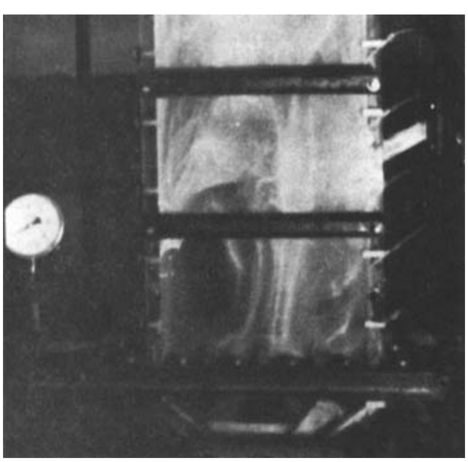

Figure 5. Macroturbulent eddies in 2D bed at $u_f = 0.443$ m/s.

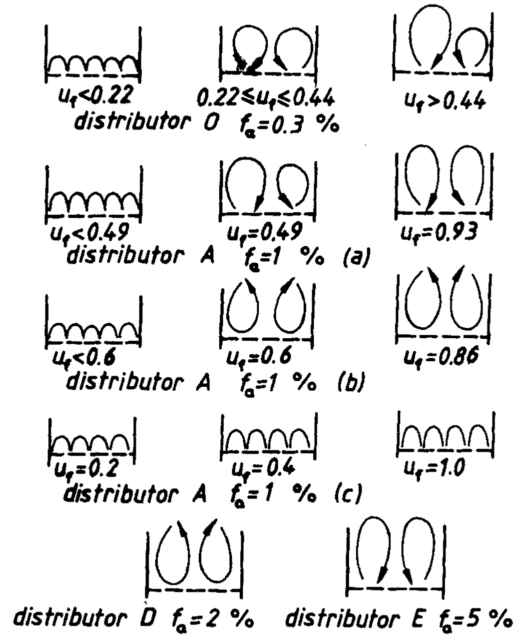

Figure 6. Simplified models of macroturbulent eddies in 2D bed.

tal section were closed. The mean residence time and the variance are determined as follows:

$$\bar{t} = \frac{\int_0^\infty t c(t)\, dt}{\int_0^\infty c(t)\, dt} \tag{2}$$

$$\sigma^2 = \frac{\int_0^\infty (t - \bar{t})^2 c(t)\, dt}{\int_0^\infty c(t)\, dt} \cdot \frac{1}{\bar{t}^2}. \tag{3}$$

The Peclet number Pe was estimated from the experimental results. Pe is defined as:

$$Pe = \frac{u_f^2}{D_E \cdot \bar{t}}. \tag{4}$$

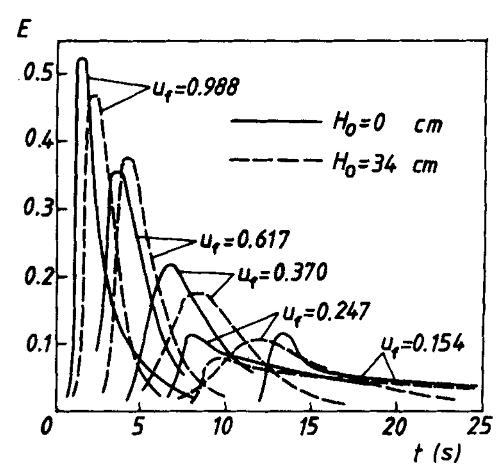

Figure 7. Gas RTD curves in 2D bed.

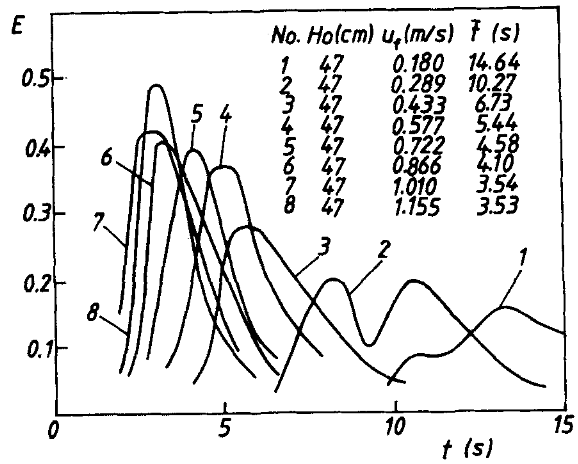

Figure 8. Gas RTD curves in 7 cm dia. bed.

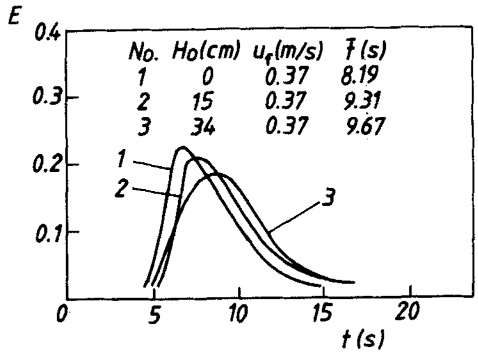

Figure 9. Comparison of gas RTD curves under various bed depths.

Simpson integration was used for calculating $\bar{t}$ and σ^2. The gas dispersion coefficient D_E vs. gas velocity data are presented in Figure 10. The curves demonstrate that D_E at low gas velocity is approximately proportional to u_f^2. This agrees with the expression of Kunii and Levenspiel (1968). As a result of an appearance of the macroturbulent eddies the value of D_E rises quickly with increasing gas velocity at $u_f = 0.4$–0.8 m/s. If $u_f \geq 0.8$ m/s, D_E will rise slowly with increasing gas velocity. At higher gas velocity the coefficient D_E decreases with increasing gas velocity, as shown by Avidan (1982). In consequence, plots of D_E vs. u_f in Figure 10 show that D_E is concerned with the bed depth and the horizontal characteristic size of bed.

Acknowledgment

The author is indebted to Mooson Kwauk for his critical review of this manuscript and his comments. The author acknowledges the assistance of Yu-jao Wang and Xi-chun Guo in constructing the measuring system, of Ji-di Yuan and Ji-fung Peng in constructing the apparatus and performing the experimental work, and of Hung Xu in performing the photographic work.

Notation

$c(t)$ = tracer concentration, mol/m^3
D = bed diameter, m

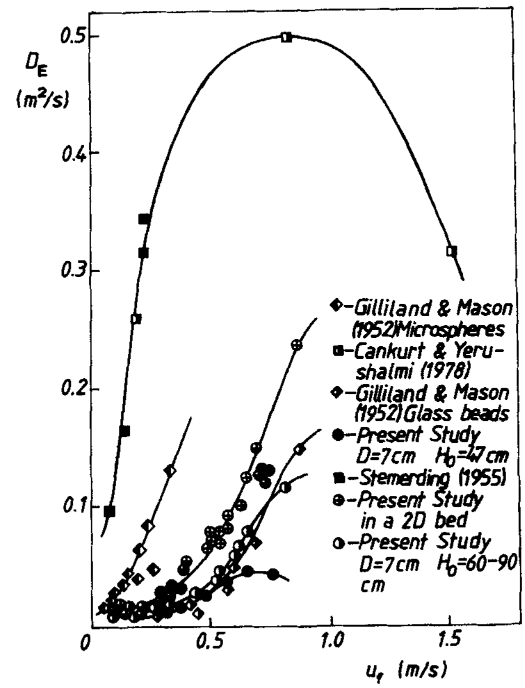

Figure 10. Gas dispersion coefficient D_E vs. gas velocity u_f.

D_E = dispersion coefficient, m^2/s
E = density function of gas RTD
f_a = free area ratio of distributor
H_o = initial bed height, m
H_t = height from distributor to sample probe, m
t = time, s
$\bar{t}$ = mean residence time of tracer in fluidized bed, s
$\bar{t}_m$ = mean residence time of tracer in measuring system, s
u_f = gas velocity, m/s

Literature Cited

Avidan, A. A., "Turbulent Fluid Bed Reactors Using Fine Powder Catalysts," *Proc. CIESC/AIChE Joint Meet. Chem. Eng.*, Beijing, China, v. 1 (Sept., 1982).

Cankurt, N. T., and J. Yerushalmi, "Gas Backmixing in High Velocity Fluidized Beds," in Fluidization (Proc. of the second Eng. Found. Conf.), J. F. Davidson and D. L. Keairns, ed., Cambridge Univ. Press (1978).

Gilliland, E. R., and E. A. Mason, "Gas and Solid Mixing in Fluidized Beds," *Ind. Eng. Chem.*, **41**, 1191 (1949).

———, "Gas Mixing in Beds of Fluidized Solids," *Ind. Eng. Chem.*, **44**, 218 (1952).

Kunii, D., and O. Levenspiel, "Bubbling Bed Model. Model Flow of Gas through a Fluidized Bed," *Ind. Eng. Chem. Fundam.*, **7**, 446 (1968).

Nguyen, H. V., A. B. Whitehead, and O. E. Potter, "Gas Backmixing, Solids Movement, and Bubble Activities in Large-scale Fluidized Beds," *AIChE J.*, **23**, 913 (1977).

Stemerding (Reman, G.H.), "Effect of Gas and Solid Mixing in Fluidized Beds on Chemical Reactions," Chem. and Ind., 46, (Jan. 15 1955).

Manuscript received Oct. 2, 1985, and revision received March 6, 1987.